# Experimental study of the crystal stability and equation of state of Si to 248 GPa

Steven J. Duclos,* Yogesh K. Vohra, and Arthur L. Ruoff
*Department of Materials Science and Engineering, Cornell University, Ithaca, New York 14853-1501*
(Received 5 February 1990)

The room-temperature equation of state of silicon, as determined from *in situ* energy-dispersive x-ray diffraction using a synchrotron source, is presented to 248 GPa. An intermediate phase between the primitive hexagonal and hexagonal-close-packed (hcp) phases is stable from 37.6±1.6 to 41.8±0.5 GPa, and is shown to be the same structure as the *X* phase of the alloy $Bi_{0.8}Pb_{0.2}$, and is *not* a simple restacking of hexagonal-close-packed layers (i.e., Sm-type, dhcp, or thcp). The hcp→fcc phase transition occurs at 79±2 GPa. The fcc phase remains stable to 248 GPa, where the silicon fractional volume is $V/V_0=0.361\pm0.006$. Excellent agreement between first-principles total-energy calculations and these results is observed for the hcp→fcc transition pressure, and the fcc Si pressure-versus-volume equation of state.

## I. INTRODUCTION

Studies of the room-temperature high-pressure phase diagram of Si have challenged both the theorist and experimentalist in recent years. The refinement of first-principles total-energy calculations has made possible the prediction of lattice structure stability as a function of volume.[1,2] These calculations also yield pressure-versus-volume equations of state (EOS), bulk moduli, and electronic properties.[3] Experimental results to 50 GPa have shown metallization at the diamond→$\beta$-Sn phase transition at 12 GPa,[4–8] the first elemental primitive hexagonal (ph) phase (Refs. 9 and 8) at 16 GPa, and a hexagonal-close-packed (hcp) phase at 42 GPa.[9,8] In addition, a phase [Si(VI)] intermediate between ph and hcp has been observed by one of the two x-ray diffraction investigations that reached 50 GPa.[8] In a previous paper[10] we reported the extension of the Si EOS to 100 GPa, and the observation of a hcp→fcc phase transformation. In this paper we report further details of this transition, extend the EOS of Si to 248 GPa, and present new data on the intermediate [Si(VI)] phase of Si.

In Sec. II we present data which verify the existence of the intermediate phase between the ph and hcp structures. While the crystallographic structure of this phase remains unknown, the data clearly indicate that an expected multi-layered hexagonal structure is not the stable structure. Section III describes the hcp→fcc phase transition at 79±2 GPa, a transition which had been predicted by first-principles theories prior to the experiments. The room-temperature equation of state of silicon to 248 GPa is discussed in Sec. IV. Conclusions are drawn in Sec. V on the adequacy of the potentials used in the first-principles models. The importance of the 3*d* basis set in correctly predicting transitions in third-row simple metals is also discussed.

Data from four room-temperature high-pressure crystallography experiments are described in this paper. Throughout, the experiments will be referred to by number, as given in Table I. Some of the relevant data acquisition parameters are summarized in the table. For the anvil geometry, *a* is the central flat diameter, $\gamma$ the bevel angle, and *b* the culet diameter. All of the experiments used spring steel gaskets, and the Si was finely ground from ingots of 99.9999% purity, mixed with the Au pressure marker, if used, and packed into the sample chamber. Experiment 1 was conducted on both the hard bend magnet (*B*) and wiggler (*A*3) beam lines at the Cornell high-energy synchrotron source (CHESS) (Ithaca, NY), and experiments 2–4 were conducted entirely on the hard bend line. The energy-dispersive x-ray-diffraction (EDXD) setup used is described by Brister, Vohra, and Ruoff.[11] The pressures in experiments 1 and 3 were determined from the nonhydrostatic ruby $R_1$ luminescence calibration of Mao *et al.*[12]

## II. THE INTERMEDIATE PHASE, Si(VI)

In experiment 1 the Si(VI) phase intermediate between primitive-hexagonal and hexagonal-close packed was in-

TABLE I. Summary of the Si high-pressure, room-temperature, crystallography experiments.

| Expt. no. | Pressure marker | Pressure range (GPa) | Sample diam ($\mu$m) | Anvil geometry $a/\gamma/b$ ($\mu$m)/(deg)/($\mu$m) | Pinhole diam ($\mu$m) |
|---|---|---|---|---|---|
| 1 | ruby | 32→43→36 | 150 | Flat, $a=600$ | 50 and 80 |
| 2 | 15 wt. % Au | 0→116 | 50 | 100/10/300 | 20 and 30 |
| 3 | ruby | 71→95→68 | 50 | 100/5/300 | 20 |
| 4 | 30 wt. % Au | 133→248 | 50 | 50/7/300 | 25 |

 

vestigated. At pressures up to 36.0 GPa diffraction peaks of a pure primitive-hexagonal phase were observed. Figure 1(c) shows a typical diffraction pattern of ph Si at 36.0 GPa. A total of 19 diffraction peaks are observed to 60 keV. These data are summarized in Table II. Considerable orientation and texturing effects were observed in this sample. At 32.0 GPa during loading the intensity ratio of (001) to (100) could be varied from 0.5 to 2 by diffracting from different parts of the sample.

At least 20 new diffraction peaks appeared at 39.6 GPa, indicating a transition to a lower symmetry intermediate structure Si(VI). The transition pressure on loading is 37.6±1.6 GPa. This phase persisted until 42.2 GPa when the hcp diffraction peaks, many of which are coincident with Si(VI) diffraction peaks, strengthened in comparison to the intermediate phase peaks. The Si(VI)→hcp transition pressure on loading is 41.8±0.5 GPa. Weak diffraction peaks of the intermediate phase persisted to 43.3 GPa, the highest pressure reached in this experiment. Downloading the cell from this pressure showed hcp diffraction peaks to 40.3 GPa, and a complete transition back to Si(VI) at 39.4 GPa, for a downloading transition pressure of 39.9±0.5 GPa. There is a small (~2 GPa) hysteresis in the Si(VI)↔hcp transition. Further downloading showed a pure Si(VI) structure at 36.7 GPa and a pure primitive-hexagonal structure at 36.0 GPa. The downloading Si(VI)→primitive hexagonal transition pressure is 36.3±0.4 GPa, indicating no hysteresis in this transition, within experimental error. Observation of this phase on loading and unloading confirms that the phase is the thermodynamically stable state of Si at pressures of 37–42 GPa and room temperature.[9]

Figure 1 shows diffraction patterns of Si in the ph, Si(VI), and hcp mixed with Si(VI) phases. The data of Olijnyk[8] show only four new diffraction peaks appearing at the ph→Si(VI) transition, two of which (22.5 and 26 keV in Fig. 1) are clearly multiplets in the present data. Because of greater intensity at energies corresponding to $d$ spacings less than 1.3 Å and improved resolution, the present data provide five times as many diffraction peaks than the previous data.[8] Table III lists the $d$ spacings and relative intensities of the observed diffraction peaks of the Si(VI) phase at 40.0 GPa. Several of these peaks are common to either the ph or hcp phase. Those peaks that may be explained by ph or hcp Si, or the hcp Fe gasket, are indicated in the table. No significant changes in the relative intensities of any of the peaks in Table III were observed over the stability range of this phase, strongly indicating that these peaks are of a pure phase.

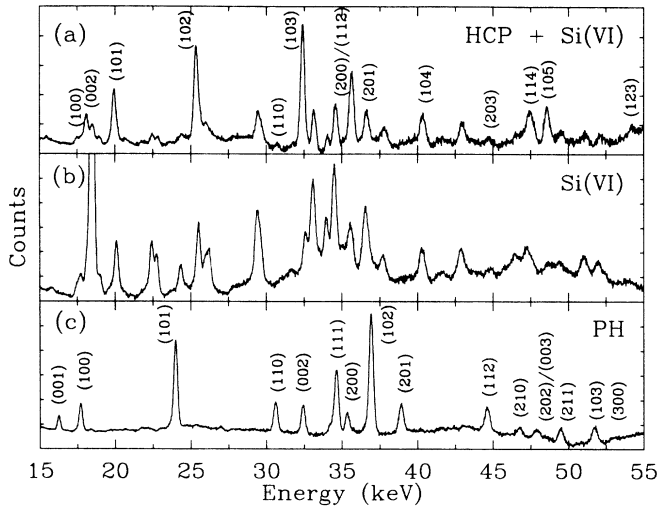


FIG. 1. Energy-dispersive diffraction spectra of silicon at room temperature. (a) Hexagonal-close-packed and Si(VI) mixtures at 42.2 GPa, (b) Si(VI) (intermediate) at 41.0 GPa, and (c) primitive hexagonal (ph) at 36.0 GPa. All three spectra were taken on the six-pole wiggler beam line at CHESS, and the diffraction constant was $Ed=37.69\pm0.02$ keV Å. A background due to Compton scattering from the diamond anvils has been numerically subtracted.

TABLE II. Observed and calculated $d$ spacings for primitive hexagonal Si at 36.0 GPa with $a=2.463$ Å. The average $\Delta d/d$ is −0.01%.

| $hkl$ | $d_{obs}$ (Å) | $d_{calc}$ (Å) | $\Delta d/d$ (%) |
|---|---|---|---|
| 001 | 2.320 | 2.325 | −0.21 |
| 100 | 2.129 | 2.133 | −0.19 |
| 101 | 1.572 | 1.572 | 0.00 |
| 110 | 1.232 | 1.232 | 0.00 |
| 002 | 1.163 | 1.163 | 0.00 |
| 111 | 1.088 | 1.088 | 0.00 |
| 200 | 1.066 | 1.067 | −0.05 |
| 102 | 1.021 | 1.020 | 0.06 |
| 201 | 0.969 | 0.969 | 0.00 |
| 112 | 0.845 | 0.845 | 0.00 |
| 210 | 0.806 | 0.806 | 0.00 |
| 202 | 0.787 | 0.786 | 0.13 |
| 003 | 0.775 | 0.775 | 0.00 |
| 211 | 0.762 | 0.762 | 0.00 |
| 103 | 0.729 | 0.728 | 0.07 |
| 300 | 0.711 | 0.711 | 0.00 |
| 301 | 0.680 | 0.680 | 0.00 |
| 212 | 0.663 | 0.663 | 0.00 |
| 113 | 0.656 | 0.656 | 0.00 |

Despite these improvements in the data quality, it has not been possible to index these energy-dispersive patterns to a structure. A systematic search was conducted over tetragonal, orthorhombic, monoclinic, and rhombohedral lattices with 1–10 atoms per unit cell, and fractional volumes between those observed for the ph and hcp phases. This search revealed only one unit cell that could explain all of the peaks unique to the intermediate phase in Table III with an error of less than 150 eV (which corresponds to 0.4% error in $d$ at $d=1.1$ Å). This cell (monoclinic, 4 atoms/cell, $V/V_0=0.561$, $a=2.351$ Å$\simeq a_{ph}$, $b=3.996\simeq\sqrt{3}a_{ph}$, $c=5.279$ Å$\simeq 2c_{ph}/\sin\gamma$, $\gamma=64.7°\simeq 60°$) fitted 22 diffraction peaks to within 137 eV (including all of the peaks in Table III that have no contamination from ph or hcp Si), but was unable to match intensities satisfactorily. Several expected strong diffraction peaks are missing from the data, and several strong diffraction peaks of the data are calculated to be very weak. While orientation effects are expected to

TABLE III. Diffraction peaks and relative intensities observed at 40.0 GPa of Si(VI) (intermediate phase). The spectrum was taken on the CHESS six-pole wiggler line [see Fig. 1(b)]. Possible interferences from the ph and hcp phases of Si, and the hcp Fe gasket are given. It is unlikely that any gasket contamination exists since the normally strong (101) diffraction peak is missing. Intensity key: w, weak; m, medium; s, strong; v, very; in order of increasing intensity, vw, w, mw, m, ms, s, vs.

| | | Possible interferences | | | | Possible interferences | | |
|---|---|---|---|---|---|---|---|---|
| $d_{obs}$ (Å) | $I$ | ph Si | hcp Si | $d_{obs}$ (Å) | $I$ | ph Si | hcp Si | hcp Fe |
| 2.160 | w | | | 1.093 | s | | | |
| 2.126 | mw | (100) | (100) | 1.075 | mw | | | |
| 2.073 | m | | (002) | 1.060 | m | (200) | (112) | |
| 2.038 | vs | | | 1.031 | ms | | (201) | |
| 1.989 | mw | | | 0.999 | mw | | | (201) |
| 1.876 | ms | | | 0.935 | m | | (104) | |
| 1.681 | s | | | 0.879 | m | | | |
| 1.656 | m | | | 0.841 | w | (112) | | |
| 1.549 | m | | | 0.811 | mw | | | |
| 1.477 | s | | | 0.797 | m | | (114) | |
| 1.454 | mw | | | 0.775 | w | (003) | | |
| 1.438 | m | | | 0.763 | w | | | |
| 1.283 | s | | | 0.739 | mw | | | |
| 1.271 | m | | | 0.725 | mw | | | (212) |
| 1.139 | s | | | 0.697 | w | | (123) | |
| 1.110 | m | | | | | | | |

affect agreement with calculated intensities, the disagreement of this structure is too great to be explained this way.

The data can, however, rule out an important class of structures for the Si(VI) phase. The disappearance of the (110) diffraction peak eliminates the possibility that the phase is simply a restacking of hexagonal-close-packed layers. Writing the ph phase as $\cdots AAA \cdots$ layering, and the hcp phase as $\cdots ABAB \cdots$ layering, it is tempting to assume that an intermediate structure would remain layered with a different ordering. The double–hexagonal-close-packed structure (dhcp) with layering $\cdots ABAC \cdots$ is one possibility, although many others exist. It will now be shown that in *all* such structures the (110) diffraction peak has nonzero calculated intensity. The intensity of the (110) peak is

$$I_{110} \propto |f_{110}|^2 = f_{\mathrm{Si}}^2 \left[ \sum_n e^{2\pi i (x_n + y_n)} \right] \left[ \sum_{n'} e^{-2\pi i (x_{n'} + y_{n'})} \right] , \tag{1}$$

where $f_{\mathrm{Si}}$ is the atomic scattering factor for Si, $n$ and $n'$ run through the atoms in the unit cell (one atom per layer), and $(x_n, y_n)$ is the atomic position within the layer which is (0,0) for an $A$ layer, $(\frac{1}{3}, \frac{2}{3})$ for $B$ and $(\frac{2}{3}, \frac{1}{3})$ for $C$. Regrouping Eq. (1)

$$I_{110} \propto f_{\mathrm{Si}}^2 \left[ n + \sum_n \sum_{n'(\neq n)} e^{2\pi i (x_n + y_n - x_{n'} - y_{n'})} \right] . \tag{2}$$

However, for the possible values of $(x_n, y_n)$ and $(x_{n'}, y_{n'})$ the exponent is either 0 or $\pm 2\pi i$, and the double sum is positive definite. Therefore, the intensity of the (110) peak is nonzero. The intralayer hexagonal lattice constant $a$ in the ph phase at 34.0 GPa just before the transition to Si(VI) is 2.469 Å, nearly the same as the $a$ lattice constant in hcp phase just after the transition from Si(VI), 2.452 Å. It is reasonable to assume that restacking for the Si(VI) phase would have a similar $a$ lattice constant, (110) $d$ spacing, and (110) diffraction energy. As shown in Fig. 1, no peak exists at this energy. Therefore, the structure cannot be a restacking of hexagonal layers.

Vijaykumar and Sikka have proposed two orthorhombic structures for Si(VI) based on the earlier diffraction data[8] and work with Sn-In and Sn-Bi alloys.[13] The first is *Pbcm* with $a = 2.412$ Å, $b = 4.701$ Å, and $c = 4.167$ Å, and the second is *Pnma* with $a = 4.698$ Å, $b = 4.163$ Å, and $c = 2.414$ Å. Both of these phases can explain only one of the two peaks at ~22.5 keV in Fig. 1(b). This peak appears as a singlet in the earlier data,[8] but is clearly a doublet in the present data. There is no other peak within 1 keV in these orthorhombic phases, so only dramatic adjustment of the lattice constant would result in an explanation of the second peak.

The $X$ phase of the $Bi_{0.8}Pb_{0.2}$ alloy has the same structure as Si(VI). Degtyareva, Ponyatovskii, and Rastorguev[14] have stabilized the $X$ phase at liquid-nitrogen temperatures by quenching from 100 °C under a pressure of 1.7 GPa, and then releasing pressure at low temperature. Upon heating to room temperature the quenched alloy decomposes to a mixture of the ε-Bi-Pb (hcp) and pure Bi phases. Figure 2 demonstrates that the structure of the $X$ phase of $Bi_{0.8}Pb_{0.2}$ is the same as that of Si(VI). The logarithms of the measured $d$ spacings have been plotted for both materials. Taking the logarithm of $d$ spacings converts a multiplicative factor between the two structures (due, for example, to a difference in unit cell volumes) to

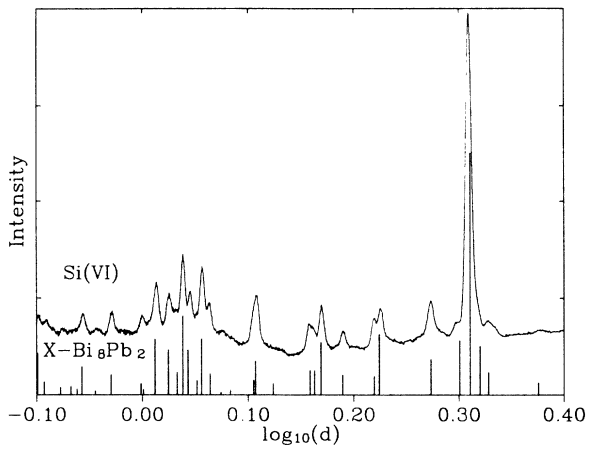


FIG. 2. Comparison of $X$-$Bi_{0.8}Pb_{0.2}$ and Si(VI) diffraction patterns. The $X$-phase data are from Degtyareva *et al.* (Ref. 14) at atmospheric pressure and liquid $N_2$ temperature. The logarithms of the $d$ spacings are plotted, and the spectra shifted to compensate for different unit cell volumes. The Si(VI) spectrum was taken on the wiggler line at CHESS.

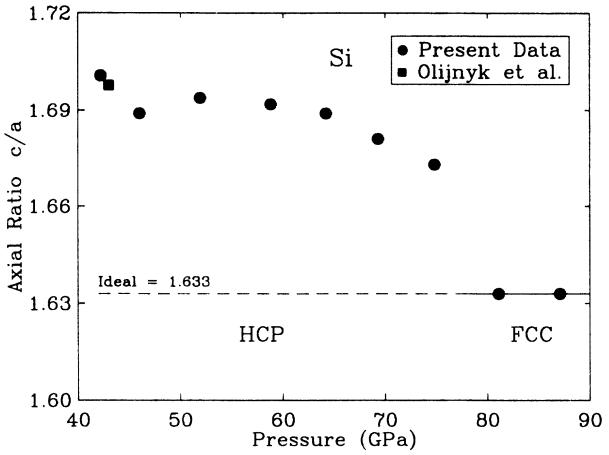


FIG. 3. Pressure dependence of the hcp silicon axial ratio $c/a$. The single data of Olijnyk *et al.* (Ref. 8) is shown with a square. The hcp→fcc transition is at 79±2 GPa.

an additive one. The two spectra have been shifted with respect to one another to maximize coincidence of diffraction peaks. The excellent match between the peaks of the two phases indicates that their structures are of the same bravais lattice with very similar axial ratios. Degtyareva *et al.*[14] tentatively assigned an orthorhombic cell to this structure, however neither the Si(VI) data nor the $Bi_{0.8}Pb_{0.2}$ data are well explained by this cell. They have suggested a monoclinic distortion,[14] but no such distortion has been found to satisfactorily explain the data.

A relatively high superconducting transition temperature $T_c \sim 8.5$–$9.0$ K has been measured[15] for $X$-$Bi_{0.8}Pb_{0.2}$. This is consistent with the $T_c$ behavior observed for Si by Erskine *et al.*[16] The anomalous increase in the Si $T_c(P)$ between 36 and 42 GPa is clearly due to the stabilization of Si(VI).

As the Pb concentration is increased, the Bi-Pb phase diagram progresses from the $X$ phase to fcc in the following manner:[15]

$$X \rightarrow \text{hcp} \rightarrow \text{fcc} \ . \tag{3}$$

As a function of pressure Si undergoes the same structure sequence, and the hcp→fcc transition will now be discussed.

### III. THE hcp→fcc TRANSITION

Experiments 1 and 2 (see Table I) provided several measurements of the hcp $c/a$ axial ratio between 42 and 75 GPa. These are plotted in Fig. 3 along with the single data point of Olijnyk *et al.*[8] The $c/a$ of 1.70 immediately after the Si(VI)→hcp transition decreases to 1.67 near the hcp→fcc transition. These data do not rule out a continuous decrease of $c/a$ to the ideal value of 1.633 at the transition, however, this would require a significantly more negative $d(c/a)/dP$ near the transition than has been observed here. The lowering of $c/a$ towards the ideal value is a precursor to the hcp→fcc transition. The agreement between the present data and that of Olijnyk *et al.*[8] is excellent. The $c/a = 1.64 \pm 0.02$ at 42 GPa measured by Hu *et al.*[7] appears to be too low, due mainly to a larger measurement of $a$. The $c/a$ behavior will be discussed in Sec. V.

Two high-pressure x-ray experiments were done to investigate the hcp→fcc transition. In experiment 2 (see Table I) the Au acted as an internal pressure marker, and pressures were calculated from the isothermal equation of state of gold by Jamieson, Fritz, and Manghnani[17] deduced from shock wave data. The gold lattice constants were determined using at least the (111), (220), and (311) diffraction peaks [and in some cases the (200) and (222)]. The results of this experiment have been briefly described earlier.[10] These results were confirmed in experiment 3 using a centered 5–10 $\mu$m ruby chip as the primary pressure sensor. In this experiment the (100), (101), (102), (110), (112), and (201) diffraction peaks of hcp Si were observed. In the fcc phase the (111), (200), (220), (311), and (222) peaks were observed. Table IV presents the indexing of fcc Si (experiment 2) at 87±7 GPa. Despite the weakness of the scatterer the average deviation of the observed $d$ spacings from the calculated ones is $-0.01\%$, comparable to that measured in high-$Z$ materials.

The observed transition pressures on compression for experiment 2 and both compression and decompression for experiment 3 are summarized in Table V. The two re-

TABLE IV. Observed and calculated $d$ spacings for fcc silicon at 87±7 GPa. The calculated $d$ spacings are based on $a = 3.341$ Å and the average $\Delta d/d = -0.01\%$.

| $hkl$ | $d_{obs}$ (Å) | $d_{calc}$ (Å) | $\Delta d/d$ (%) |
|---|---|---|---|
| 111 | 1.929 | 1.929 | 0.00 |
| 200 | 1.671 | 1.670 | 0.06 |
| 220 | 1.177 | 1.181 | −0.34 |
| 311 | 1.004 | 1.007 | −0.30 |
| 222 | 0.969 | 0.964 | 0.51 |

TABLE V. Summary of hcp↔fcc silicon transition pressures at room temperature. For the experimental details see Table I.

| | Experiment 2 | Experiment 3 |
|---|---|---|
| Pressure (GPa) of last compression spectrum showing very weak or no fcc Si | 74.0 | 77.5 |
| Pressure (GPa) of first compression spectrum showing fcc Si | 81.1 | 82.0 |
| Pressure (GPa) of last decompression spectrum showing very weak or no hcp Si | | 83.0 |
| Pressure (GPa) of first decompression spectrum showing hcp Si | | 77.0 |

sults on compression are consistent and yield 79±2 GPa for the hcp→fcc transition pressure. The ruby experiment (experiment 3) yielded 80±3 GPa for the downloading pressure. Within experimental error there is no hysteresis in this transition.

## IV. THE Si EQUATION OF STATE TO 248 GPa

Experiment 4 extended the Si fcc equation of state to 248 GPa. The concentration of the Au pressure marker was double that in experiment 2 in order to bring the Au diffraction peaks to the same intensity as the Si peaks. Several attempts were made to load the sample with a gasket thickness of 248 μm preindented to 25–30 μm thick and 25 or 50 μm sample hole. However, each resulted in unacceptably weak diffraction due to severe thinning of the sample by the 50 μm flats. Successful diffraction was obtained with a 375 μm thick spring-steel gasket preindented to 60 μm starting thickness. The initially 50 μm diameter sample expanded to at least 200 μm diameter; however, this did not significantly diminish the pressure-generating capability of the diamond-anvil cell (DAC).

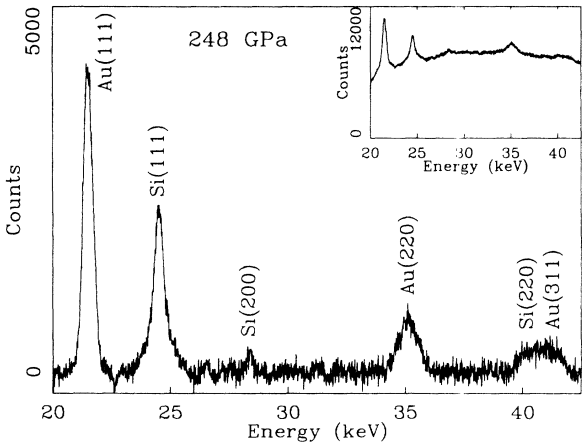


FIG. 4. EDXD spectrum of fcc Si at 248 GPa. The spectrum was taken on the *B* beam line at CHESS with a diffraction constant of $Ed = 43.42 \pm 0.03$ keV Å. A background due to Compton scattering from the diamond anvils has been numerically subtracted in the main figure, but not in the inset.

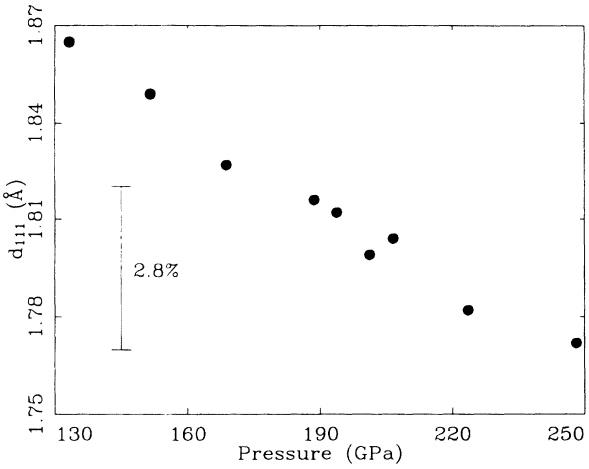


FIG. 5. Pressure dependence of the *d* spacing of the diffraction peak indexed as the (111) of fcc Si. The vertical bar indicates the 2.8% decrease in *d* expected if the structure had transformed to bcc with no atomic volume change. If there was a volume decrease the drop would be even greater.

Figure 4 shows an EDXD spectrum of fcc Si and fcc Au at 248 GPa. Because of expansion of the sample hole there is no Fe gasket contamination in this spectrum. The (111), (200), and (220) diffraction peaks of Si are observed, as are the (111), (220), and (311) diffraction peaks of Au. The (200) peak of Au is overwhelmed by the (111) peak of Si, and is not observed at this pressure. The three peaks of Si fit the fcc structure with $(d_{\text{calc}} - d_{\text{obs}})/d_{\text{obs}}$ less than 0.3% for each peak, and for Au the fitting error is less than 0.04% for each peak. For both materials the

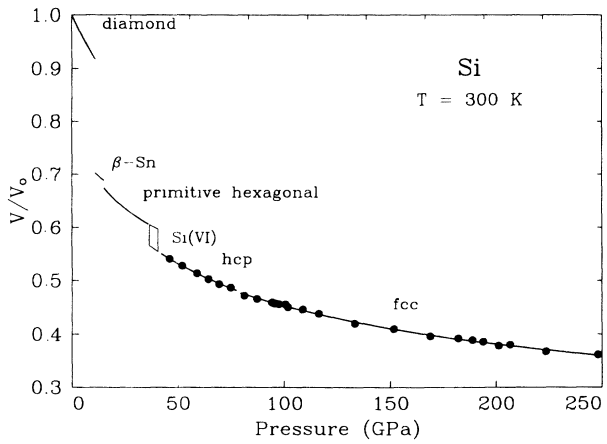


FIG. 6. The room-temperature equation of state of Si to 248 GPa. The solid circles are the data obtained in the present work. The solid lines are Birch first-order EOS fits to the data. For the diamond, β-Sn, and ph EOS data see Olijnyk *et al.* (Ref. 8). The box at approximately 40 GPa indicates the region in which Si(VI) is expected to be stable. A hcp→fcc transition occurs at 79±2 GPa.

TABLE VI. The Birch equation of state parameters for hcp and fcc Si. $V_n/V_0$ is the fractional volume of the phase extrapolated back to atmospheric pressure. The fcc theory values are from the LMTO equation of state of McMahan and Moriarty (Refs. 1 and 20).

| | hcp | fcc | fcc theory |
|---|---|---|---|
| $V_n/V_0$ | 0.754±0.005 | 0.716±0.008 | 0.72 |
| $B_0$ (GPa) | 72±2 | 82±2 | 94 |
| $B_0'$ | 3.91±0.07 | 4.22±0.05 | 4.17 |

(111) peak intensity is much greater than that of any other peak, and therefore dominates the weighted fit of the lattice parameter.

One important question to answer is whether Si has transformed to the (bcc) phase within the pressure range of this study. The (110) diffraction peak, the strongest of bcc, falls very close to the (111) of fcc if the volume change is small. For no change in the volume per atom $a_{\rm fcc}^3 = 2a_{\rm bcc}^3$, and the energy ratio of the two peaks is

$$\frac{E_{(110)\ \rm bcc}}{E_{(111)\ \rm fcc}} = \frac{d_{(111)\ \rm fcc}}{d_{(110)\ \rm bcc}} = \frac{\sqrt{2}a_{\rm fcc}}{\sqrt{3}a_{\rm bcc}} = \frac{2^{5/6}}{\sqrt{3}}\frac{a_{\rm bcc}}{a_{\rm bcc}} = 1.028 . \quad (4)$$

Any decrease in volume of the transition would increase this number. Therefore, at the transition at least a 2.8% increase in the energy of the strongest diffraction peak is expected, or at least a 2.8% decrease in its $d$ spacing. Figure 5 shows that such a decrease has clearly not occurred between 130 and 248 GPa. This, in addition to the excellent agreement to three fcc diffraction peaks, leads to the conclusion that Si is stable in the fcc phase to at least 248 GPa.

The equation of state of Si to 248 GPa is shown in Fig. 6. The bulk moduli, their pressure derivatives, and fractional volume extrapolated to atmospheric pressure for the hcp and fcc phases are presented in Table VI. The fractional volume of hcp Si at the hcp→fcc transition is 0.480. At the transition there is a 0.003 decrease in $V/V_0$ to 0.477. This decrease is smaller than the estimated error in $V/V_0$ measurements of ±0.006, so the possibility of no volume change at the transition cannot be ruled out. At 248 GPa the fractional volume of Si is 0.361, giving a nearest-neighbor distance of 2.17 Å, which is 7.7% less than at atmospheric pressure. The bulk modulus of Si is 890 GPa at 248 GPa, nearly twice the atmospheric pressure bulk modulus of (carbon) diamond.

## V. DISCUSSION

Several theoretical predictions of the hcp→fcc transition were made prior to these experiments. For each a different technique was used to calculate the total crystal energy of the static lattice, $E$ consisting of the electronic kinetic energy, Coulombic electron-electron energy, electronic exchange and correlation energy, and the ionic (core-core) Coulomb energy.[18] Calculations were done for each plausible crystal structure as a function of atomic volume. At a given volume the structure with the lowest total energy is the stable structure. Strictly speaking it is the difference in Gibbs free energy $\Delta G$ at fixed pressure that will determine crystal stability; however, Moriarty[1,19] has shown that for the close-packed structures of Si the leading correction to $\Delta G = \Delta E$ is about 1% of $\Delta E$ itself.

The three techniques used to calculate $E$ and predict the hcp→fcc transitions in Si are the linear muffin-tin orbital (LMTO) method,[1] the generalized pseudopotential theory[1] (GPT), and the *ab initio* pseudopotential (AP) theory.[2] All three include $s$, $p$, and $d$ state electronic contributions, use the local-density-functional formulation for the exchange and correlation energy, ignore zero-point energies, and are strictly appropriate for $T=0$ K since entropy differences are not considered.[1,2] The AP theory uses a rigid (frozen) Ne-like core, whereas GPT core states are volume dependent, and the LMTO self-consistently treats all but the $s$ states as band states in the atomic-sphere approximation. Test calculations have shown that even at tenfold compression the $f$ states have a negligible contribution to $E$ in Si.[1]

Table VII compares the predicted transition parameters (pressure, fractional volume, and fractional volume change) to the measured ones. All three theories correctly predict the stability of the fcc phase. There is remarkable agreement between the measured and predicted transition pressures and transition volumes of the LMTO calculations of McMahan and Moriarity.[1] The AP predicted pressure and volume appear to be high and low, respectively.[2] A possible explanation for the discrepancy is the frozen-core approximation of the AP theory. Tests up to twofold compression have shown that this approximation is a good one;[1] however, the hcp→fcc transition occurs beyond twofold compression. The disagreement with the experiment indicates further testing of the frozen-core approximation may be needed. Success of the LMTO calculation stems from the fact that the charge distributions of these close-packed metallic structures are nearly spherical about the ions. Therefore, the LMTO atomic-sphere approximation can closely approximate the expected charge distribution.

The theoretical success allows us to physically interpret the driving mechanism for close-packed structure transitions for high-density, third-period metals. The transition results from the lowering and filling of the orig-

TABLE VII. Comparison of predicted and measured hcp→fcc transition parameters for silicon. The GPT and LMTO predictions are from McMahan and Moriarty (Ref. 1), and the AP predictions are from Chang and Cohen (Ref. 2). The GPT and LMTO transition pressures are from the LMTO equation of state (Ref. 20).

| | | Transition fractional volume ($V/V_0$) | Fractional volume change | Pressure (GPa) |
|---|---|---|---|---|
| Theory | GPT | 0.482 | | 88 |
| | LMTO | 0.496 | | 77 |
| | AP | 0.465 | 0.009 | 116 |
| Present experiments | | 0.481±0.005 | 0.003±0.006 | 79±2 |

inally empty $3d$ band as the density and coordination number (CN) is increased.[1] As the CN is increased at a given volume, the nearest-neighbor distance also increases generating a less localized charge density. Such delocalization weakens the covalent bonding, and it results in a lowering of the $3d$-band energy as charges move to interstitial regions. Lowering of the $3d$ electronic band energy is closely connected to the energetics of transitions between the high coordination number (CN of 12) close-packed structures. In fact, McMahan and Moriarity[1] have found that when the $3d$ basis states are eliminated from the LMTO calculation no transition from hcp is predicted down to $V/V_0=0.07$.

The hcp structure axial ratio, $c/a$, and its pressure dependence provides another test of these total-energy theories. At a given crystal volume the $c/a$ ratio can be varied in the model calculations, and an equilibrium value for which $E$ is minimized can be found. At a volume corresponding to the hcp structure just after the transition from Si(VI) the GPT predicts[1] $c/a=1.67$, and the AP theory[2] $c/a=1.695$. The AP value is in excellent agreement with the experiment, as shown in Fig. 3. The GPT, at more than twofold compression, may require less localized $d$ basis states for a more accurate calculation of $c/a$, as had been suggested before the experiment.[1]

Chang and Cohen[2] have shown that in the ph phase of Si the bonding is stronger between the hexagonal layers due to a pile up of covalent charge in the axial direction. This is manifested experimentally by an increasing $c/a$ ratio as pressure is increased in the ph phase.[8] The present data (see Fig. 3) indicate the opposite is true for the hcp phase. As a function of pressure the electronic charge density is reduced between the layers, resulting in weaker bonds; so much so that in this phase $c/a$ decreases with pressure. This $c/a$ decrease towards the ideal (fcc) ratio is likely to reduce the energy barrier of the hcp→fcc transition.

The theories of McMahan and Moriarty[1] have been used to predict a fcc to bcc structure transition at higher pressures. The GPT predicts this transition at $V/V_0\sim0.18$, $P\sim2800$ GPa, and the LMTO at $V/V_0\sim0.155$, $P\sim3600$ GPa.[20] No transition to bcc has been observed in Si to 248 GPa, consistent with the theoretical predictions. Further, the measured fractional volume of Si at 248 GPa, $0.361\pm0.006$, is in good agreement with the LMTO equation of state calculation of $V/V_0=0.374$ at 248 GPa.[20]

Finally, the complete picture of transitions of Si from diamond structure to fcc invites a comparison to the transitions in Ge. This is shown in Table VIII. Ge has been studied to 125 GPa (Ref. 21) and shows three phase transitions at room temperature. The first two are the same as the first two in Si, diamond→$\beta$-Sn→ph, while the third requires further investigation, but is similar to Si in that ph does not directly transform to hcp. The two metallic Ge transitions, $\beta$-Sn→ph and ph→intermediate, require considerably larger pressures than their counterparts in Si. This results from the filled $3d$ band in Ge exerting a Pauli repulsion on the $d$ character valence electrons which are created as the originally empty $4d$ states are lowered with pressure in a manner similar to the $3d$ states in Si. For a given structure this repulsion increases $|\partial E_{\rm tot}/\partial V|$, and therefore the pressure, at volumes comparable to the transition volumes.[18] Therefore, the common tangents of $E_{\rm tot}(V)$ for the metallic structures are larger in Ge, resulting in the larger transition pressures seen in Table VIII.

TABLE VIII. Comparison of Si and Ge transition pressures at room temperature. As with Si, the intermediate phase of Ge has not been identified. Diffraction spectra of the two materials, while similar, do not rule out the possibility that the intermediate phase of Ge is different than that of Si(VI).

| Phase | Transition pressure (GPa) Si | Ge |
|---|---|---|
| diamond→$\beta$-Sn | 12[a] | 10.6[b] |
| $\beta$-Sn→ph | 16[a] | 75[c] |
| ph→intermediate | 36 | 102[c] |
| intermediate→hcp | 42 | |
| hcp→fcc | 79 | |

[a]See Hu and Spain (Ref. 9).
[b]See Menoni, Hu, and Spain (Ref. 22).
[c]See Vohra *et al.* (Ref. 21).

## VI. CONCLUSIONS

We have shown that the Si(VI) phase, intermediate between the ph phase and hcp phase, is a stable structure of Si. Disappearance of the hexagonal (110) diffraction peak indicates that the structure is not simply a relayering of basal planes, such as occurs in the dhcp structure. Si(VI) does have the same structure as $X$-$Bi_{0.8}PB_{0.2}$ which is obtained after pressure and temperature quenching of the alloy. The anomolous behavior of the pressure dependence of the Si superconducting $T_c$ is explained by the stability of this phase.

At room temperature the hcp→fcc transition in Si occurs at $79\pm2$ GPa and fractional volume of $0.481\pm0.005$. It is preceded by a decrease in the hcp $c/a$ axial ratio, and an approach to the ideal hcp value. The volume discontinuity at the transition is very small, $\Delta V/V_t=0.003$, and a continuous transition in volume cannot be ruled out. First-principles total-crystal-energy calculations are shown to be successful in predicting the stability of the fcc phase for high-density Si, with generally good agreement to the measured transition pressure. The fractional volume of Si at 248 GPa is measured to be 0.361, in reasonable agreement with a first-principles LMTO calculation result[1,20] of 0.374.

## ACKNOWLEDGMENTS

We thank Keith Brister, Sam Weir, Serge Desgreniers, and Hui Xia for their assistance at CHESS. Also, helpful discussions with A. K. McMahan are gratefully acknowledged. One of us (S.J.D.) thanks AT&T Bell Laboratories for support. This work received support from National Science Foundation (NSF) through Grant No. DMR-861-12289.

*Present address: AT&T Bell Laboratories, Murray Hill, New Jersey 07974-2070.

[1]A. K. McMahan and John A. Moriarty, Phys. Rev. B **27**, 3235 (1983).

[2]K. J. Chang, and Marvin L. Cohen, Phys. Rev. B **31**, 7819 (1985).

[3]Amy Y. Liu, K. J. Chang, and Marvin L. Cohen, Phys. Rev. B **37**, 6344 (1988).

[4]F. P. Bundy, J. Chem. Phys. **41**, 3809 (1964).

[5]B. Welber, C. K. Kim, Manuel Cardona, and Sergio Rodriguez, Solid State Commun. **17**, 1021 (1975).

[6]M. C. Gupta and A. L. Ruoff, J. Appl. Phys. **51**, 1072 (1980).

[7]Jing Zhu Hu, Larry D. Merkle, Carmen S. Menoni, and Ian L. Spain, Phys. Rev. B **34**, 4679 (1986).

[8]H. Olijnyk, S. K. Sikka, and W. B. Holzapfel, Phys. Lett. **103A**, 137 (1984).

[9]J. Z. Hu and I. L. Spain, Solid State Commun. **51**, 263 (1984).

[10]Steven J. Duclos, Yogesh K. Vohra, and Arthur L. Ruoff, Phys. Rev. Lett. **58**, 775 (1987).

[11]Keith E. Brister, Yogesh K. Vohra, and Arthur L. Ruoff, Rev. Sci. Instrum. **57**, 2560 (1986).

[12]H. K. Mao, P. M. Bell, J. W. Shaner, and D. J. Steinberg, J. Appl. Phys. **49**, 3276 (1978).

[13]V. Vijaykumar and S. K. Sikka (unpublished).

[14]V. F. Degtyareva, E. G. Ponyatovskii, and L. N. Rastorguev, Fiz. Tverd. Tela (Leningrad) **17**, 439 (1975) [Sov. Phys.—Solid State **17**, 274 (1976)].

[15]V. F. Degtyareva and E. G. Ponyatovskii, Fiz Tverd. Tela (Leningrad) **24**, 2672 (1982) [Sov. Phys.—Solid State **24**, 1514 (1982)].

[16]David Erskine, Peter Y. Yu, K. J. Chang, and Marvin L. Cohen, Phys. Rev. Lett. **57**, 2741 (1986).

[17]J. C. Jamieson, J. Fritz and M. H. Manghnani, Adv. Earth Planet. Sci. **12**, 27 (1980).

[18]M. T. Yin and Marvin L. Cohen, Phys. Rev. B **26**, 5668 (1982).

[19]J. A. Moriarity, Phys. Rev. B **8**, 1338 (1973).

[20]A. K. McMahan (private communication).

[21]Y. K. Vohra, K. E. Brister, S. Desgreniers, A. L. Ruoff, K. J. Chang, and M. L. Cohen, Phys. Rev. Lett. **56**, 1944 (1986).

[22]Carmen S. Menoni, Jing Zhu Hu, and Ian L. Spain, Phys. Rev. B **34**, 362 (1986).